International Journal of Heat and Mass Transfer 54 (2011) 983–993

Contents lists available at ScienceDirect

International Journal of Heat and Mass Transfer

journal homepage: www.elsevier.com/locate/ijhmt

# Semi-analytical method for heat and moisture transfer in packed bed of silica gel

A. Ramzy K, T.P. Ashok Babu, Ravikiran Kadoli *

*Mechanical Engineering Department, National Institute of Technology Karnataka, Surathkal, Mangalore, India*

ARTICLE INFO

*Article history:*
Received 18 May 2009
Received in revised form 24 March 2010
Accepted 1 September 2010
Available online 11 November 2010

*Keywords:*
Adsorption
Desorption
Silica gel
Desiccants
Dehumidification
Packed bed

ABSTRACT

A semi-analytical model for the heat and mass transfer of adsorption and desorption processes of the vertical solid desiccant packed bed dehumidifier is presented on the basis of quasi-steady state assumption, and is solved using close form integration with the limits equivalent to bed and time increments, and numerically by Runge–Kutta Fehlberg and forward scheme finite difference techniques. The most important parameters during the dehumidifier operation, namely, (i) exit air temperature and humidity, (ii) axial temperature distribution in the bed and (iii) water content are evaluated. Stability of the semi-analytical method is investigated and found that the main parameters affecting the model stability are the bed and time increments size. A dimensionless parameter combining time and bed increments size and air velocity named velocity ratio is defined and investigated. It is found that when the velocity ratio equals the ratio of particle diameter to bed length, the method is stable, and as the velocity ratio is made smaller beyond the stable velocity ratio, the results remain unchanged. The results of semi-analytical and numerical models agree well with the experimental results for both desorption and adsorption processes. Using the proposed semi-analytical model, the minimum and maximum relative errors for exit air temperature are 2.24% and 11.78%, respectively and for exit air humidity the minimum and maximum errors are 3.79% and 27.17% respectively.



## 1. Introduction

Adsorption of gases and vapors by micro, macro and mesoporous solids has attracted much attention because of its practical interests in the fields of gas separation (Cruz et al. [1]), purification (Esteves and Mota [2]), air conditioning (Daou et al. [3]) and refrigeration (Sumathy et al. [4] and Kim and Ferreira [5]). For environment friendly air conditioning purposes, desiccant based dehumidification system provides a great interest due to global warming problems, and offers a promising alternative to conventional air-conditioning, specially under conditions involving high latent loads. In desiccant cooling systems, the process air is dehumidified and then cooled before being sent to the conditioned space. Desiccants remove moisture from the supply air until they reach a state at which it cannot give the required air quality. The heat of adsorption released in the process heats up the supply air. To run the dehumidification system continually, the adsorbed water vapor must be rejected from the desiccant material (silica gel, zeolites) by heatless or thermal desorption processes such that desiccant materials can adsorb the required water vapor in the next cycle. Heatless desorption process is achieved by exposing the bed to the air stream with very low water vapor pressure, and thermal desorption takes place by heating up the desiccant material with a regenerative air stream or directly exposing the bed to a hot air stream. In general, the regeneration temperature for silica gels is less than that of zeolites (Chang et al. [6]) and is as low as 50 °C (Ng et al. [7]). Moreover silica gel is a hydrophilic desiccant. Therefore, silica gel is used in this study as the desiccant material in the packed bed.

The physical properties of silica gel were studied and reported by many investigators [7,8]. The related theoretical works in physical adsorption were summarized in detail by Yang [9]. The uptake curve of a constant-volume sorption system with two coupled intra-particle mass diffusion resistances was obtained by Ma and Lee [10] and Lee [11]. Two limiting cases of the solution, individually corresponding to the macro-pore and micro-pore diffusion controlled systems were obtained. Some work for adsorption in packed bed was performed. An analytical solution for diffusion process in a spherical adsorbent particle with both thermal effect and external gas-side mass transfer resistance in an adsorption process was obtained by Ni and San [12]. A uniform temperature distribution was assumed in the adsorbent particle, and the solid side resistance model was employed for the moisture balance of the system. The adsorbate concentration in the solid was obtained by solving the governing equations using Laplace transformation. Awad et al. [13] and Ramzy et al. [14] studied the heat and mass transfer in radial flow hollow cylindrical packed bed for both single blow test adsorption or desorption process and cyclic operation.

* Corresponding author.
*E-mail addresses:* ahmed_ara1979@mans.edu.eg (A. Ramzy K), tpashok@rediffmail.com (T.P. Ashok Babu), rkkadoli@nitk.ac.in (R. Kadoli).

0017-9310/$ - see front matter © 2010 Elsevier Ltd. All rights reserved.
doi:10.1016/j.ijheatmasstransfer.2010.09.007

**Nomenclature**

| | |
|---|---|
| $A$ | bed cross section area [$m^2$] |
| $a_s$ | surface area per unit volume of the bed [$m^{-1}$] |
| Ads | adsorption process |
| $C$ | specific heat [kJ/kg K] |
| $D$ | diffusion coefficient [$m^2$/sec] |
| $d$ | diameter [m] |
| Des | desorption process |
| $dv$ | incremental volume [$m^3$] |
| $f$ | fluid friction coefficient |
| $G$ | mass flux [kg/$m^2$ sec] |
| $h$ | heat transfer coefficient [W/$m^2$.K] |
| $H_A$ | heat of adsorption [kJ/kg] |
| $h_m$ | mass transfer coefficient [kg/$m^2$.sec ] |
| ID | intermediate density silica gel |
| $k$ | conductivity [W/m sec] |
| $L$ | length of bed [m] |
| $\dot{m}$ | mass flow rate [kg/s] |
| $n$ | number of bed layers |
| $NTU_h$ | number of unit transfer of heat $[ha_sA\Delta z/\dot{m}]$ |
| $NTU_m$ | number of unit transfer of mass $[h_m a_s A\Delta z/\dot{m}]$ |
| $P$ | pressure [Pa] |
| $p$ | passage thickness [m] |
| $q$ | gel water content [$kg_w$/$kg_s$] |
| $r$ | radius |
| RD | regular density silica gel |
| $Re$ | reynolds number |
| $RH$ | relative humidity [%] |
| $RT$ | relative time |
| $T$ | temperature [°C] |
| $t$ | time [sec] |
| $v$ | superficial velocity [m/s] |
| $VMTR$ | volumetric mass transfer rate [kg/$m^3$sec] |
| $w$ | humidity ratio [$kg_v$/$kg_a$] |
| $z$ | axial position in the bed [m] |

*Subscripts*

| | |
|---|---|
| $0$ | initial value |
| $a$ | air side |
| $b$ | bed |
| $i$ | inlet |
| $j$ | time step counter |
| $n$ | number of experimental data |
| $o$ | outlet |
| $p$ | particle |
| $pe$ | pore of silica gel |
| $s$ | silica gel, desiccant particle surface |
| $sat$ | saturation |
| $tot$ | total |
| $v$ | water vapor |
| $w$ | water |

*Greek*

| | |
|---|---|
| $\rho$ | density [kg/$m^3$] |
| $\varepsilon$ | porosity |
| $\delta(X)$ | root of mean square of relative error |
| $\psi$ | velocity ratio |
| $\Delta$ | incremental change |

The governing equations were derived considering gas side resistance and lumped capacitance method for the mass and energy balances and the model was solved numerically and verified with experimental data. San and Jiang [15] applied the solid-side resistance model in analyzing the adsorption performances of a packed bed in a periodic steady-state operation, where the friction effect was added to the energy balance equation. The numerical results were compared with the experimental data and a good agreement was obtained. Pesaran and Mills [16,17] established a solid-side resistance model for analyzing the adsorption of water vapor on silica gel in a packed bed and the governing equations were solved numerically. The same solid side resistance model was solved numerically by Kafui [18] for packed bed and parallel passage matrix of silica gel by considering the temperature distribution inside the spherical particles.

In this study, the mathematical model for heat and moisture transfer in a silica gel packed bed is described and analyzed, which considers the effects of fluid friction, the axial distribution of bed temperature and the amount of water content on the porous desiccant materials during and after the adsorption/desorption processes. A lumped capacitance method is adopted for the energy and moisture balances. The set of coupled governing differential equations describing the adsorption and desorption processes in the dehumidifying bed is solved using (i) a semi-analytical method based on the quasi-steady state assumption, and (ii) numerically using Runge–Kutta Fehlberg and forward scheme finite difference techniques. In the semi-analytical approach the governing equations are solved by close form integration. It is found that when the limits of integration are the total bed length and operation time, the transient axial distribution of the system parameters namely (i) air temperature and humidity and (ii) bed water content and temperature do not play any role, and hence the integrated solution are highly erroneous. For a reasonably acceptable solution, it is found that the limits of integration namely the bed and time increments ($\Delta z$ and $\Delta t$) must be arrived at properly. These increments size are embodied in a dimensionless parameter called velocity ratio. In the present work, for stable and acceptable solution numerical experiments have been conducted to identify the velocity ratio. The mechanism of various processes in the dehumidifying bed is also explained.

## 2. Theoretical model

The physical model for the silica gel packed bed is illustrated in Fig. 1(a). In packed beds of adsorbing material, air loses a part of its moisture content to the particles in a transient heat and moisture transfer process.

Adsorption/desorption processes are accompanied by the significant heat source/sink and they lead to the strong coupling between heat and mass transfer. The amount of the adsorbable species adsorbed in the bed depends on the temperature at the solid particle surface. The heat transfer by convection between the solid adsorbent particles and the air could influence greatly the local equilibrium conditions and needs to be accounted for adequate description of the adsorption process. A theoretical model for the combined heat and mass transfer in conjunction with adsorption/desorption in the vertical packed bed is presented by considering a packed bed that consists of spherical silica gel particles with uniform temperature $T_{s0}$ and initial average uptake $q_0$. The packed bed is in equilibrium with the adjacent air layer having water content of $w_{s0}$ and is suddenly exposed to humid air with water vapor mass fraction $w_{a(i,t)}$. This system is shown in Fig. 1(a). Fig. 1(b) shows bed and air conditions on the time and volume increments, and that the air humidity and temperature are varying over the incremental volume and time. Also, the bed water content and temperature are changing over the time increment and it can be stated that every

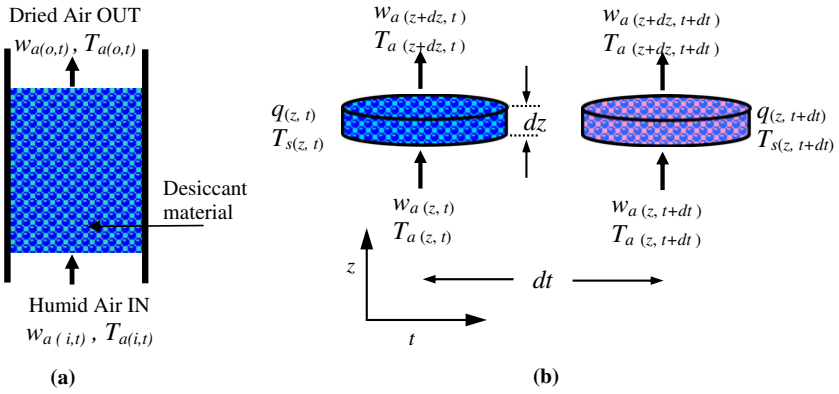


**Fig. 1.** Schematic of the adsorptive packed bed (a), and Physical model of the bed for semi-analytical solution (b).

incremental volume has an individual bed water content and temperature which depends on the flowing air state. Water vapor is transferred from the bulk air stream to particles by convective mass transfer at a rate of volumetric mass transfer rate (*VMTR*) which is calculated from

$$VMTR = h_m a_s (w_a - w_s) \tag{1}$$

where $w_s$ is calculated from the water vapor-silica gel isotherm and is given as a function of gel water content and temperature as well,

$$w_s = f(q, T_s) \tag{2}$$

The process of moisture adsorption on the surface of the silica gel particles releases an amount of heat called heat of adsorption ($H_A$), which results in bed temperature rise. Therefore adsorption and desorption process can be treated as a transient heat and mass transfer problem, and the following assumptions will be considered in the system analysis.

1. The bulk air stream contains water vapor as the only one adsorbable component.
2. Heat of adsorption results from the condensation of water vapor in the internal pores in the silica gel particles, so the heat of adsorption is assumed to be totally generated in the silica gel particles (Kamiuto and Ermalina [19]).
3. The pressure drop across the bed is small. This assumption holds true provided that the length of the bed is less than 0.15 m (Pesaran and Mills [16,17] and Kafui [18]).

Governing equations for the adsorption and desorption processes in silica gel packed beds are as follow. The species conservation equation in the gas phase

$$D_a \rho_a A \frac{\partial^2 w_a}{\partial z^2} dz - \frac{\partial(\dot{m}_a w_a)}{\partial z} dz - VMTR \times dv = \varepsilon_b dv \frac{\partial(\rho_a w_a)}{\partial t} \tag{3}$$

While overall mass conservation requires that

$$\varepsilon_b dv \frac{\partial \rho_a}{\partial t} + \frac{\partial \dot{m}_a}{\partial z} dz = -VMTR \times dv \tag{4}$$

Combining Eqs. (3), (4) and (1) results in

$$D_a \rho_a A \frac{\partial^2 w_a}{\partial z^2} dz - \dot{m}_a \frac{\partial w_a}{\partial z} dz - h_m a_s (w_a - w_s)(1 - w_a) \times dv = \varepsilon_b \rho_a dv \frac{\partial w_a}{\partial t} \tag{5}$$

In this equation, the first term in the left hand side attributes the dispersion in axial direction through the inter particle air (air between particles). The second and third are change of flowing air humidity and net convective mass transfer to the bed respectively. The right hand side is the storage term in the inter particle air. For solid phase, if intra-particle diffusion is considered, the species conservation equation for the desiccant particle can be presented as

$$\rho_s \frac{\partial q}{\partial t} + \rho_r \varepsilon_p \frac{\partial w_{pe}}{\partial t} = \frac{D_{pe} \rho_{pe}}{r^2} \frac{\partial}{\partial r}\left(r^2 \frac{\partial w_{pe}}{\partial r}\right) + \frac{D_{se} \rho_s}{r^2} \frac{\partial}{\partial r}\left(r^2 \frac{\partial q}{\partial r}\right) \tag{6}$$

where $w_{pe}$ is the humidity ratio of air in the pore and in equilibrium with the local silica gel water content and temperature, and is calculated from the silica gel isotherm ($w_{pe} = f(q_{(r,z)}, T_s)$). The left hand side, in Eq. (6), is the storage term in the desiccant particle, and the right hand side attributes both pore as well as surface diffusion rates (Ni and San [12]). Eqs. (5) and (6) are coupled by the continuity at the particle surface

$$-D_{pe} \rho_{pe} \frac{\partial w_{pe}}{\partial r}\Big)_{r=D_p/2} - D_{se} \rho_s \frac{\partial q}{\partial r}\Big)_{r=D_p/2} = h_m (w_{pe} - w_a) \tag{7}$$

The second boundary condition for Eq. (6) is as follow

$$-D_{pe} \rho_{pe} \frac{\partial w_{pe}}{\partial r}\Big)_{r=0} - D_{se} \rho_s \frac{\partial q}{\partial r}\Big)_{r=0} = 0 \tag{8}$$

Eqs. (6)–(8) can be replaced by the lumped capacitance model. The conservation of species in the solid phase is given by

$$\rho_b dv \frac{\partial q}{\partial t} = VMTR \times dv \tag{9}$$

Substituting *VMTR* and dividing by *dv* Eq. (9) can be simplified as

$$\rho_b \frac{\partial q}{\partial t} = h_m a_s (w_a - w_s) \tag{10}$$

Eq. (10) has the initial condition as

$$q_{(z,t=0)} = q_0 \tag{11}$$

The energy balance for gas phase gives

$$\varepsilon_b \rho_a C_a \frac{\partial T_a}{\partial t} dv = -\dot{m}_a C_a \frac{\partial T_a}{\partial z} dz + C_v VMTR \times (T_a - T_s) dv + h a_s (T_s - T_a) dv + \left(\frac{\dot{m}_a}{2}\right)\left(\frac{G_a}{\rho_a \varepsilon_b}\right)^2 \left(\frac{a_s f}{\varepsilon_b A}\right) dv \tag{12}$$

where, the fourth term in the right hand side attributes to the fluid friction effect in the column added by San and Jiang [15]. Eq. (12) is rearranged as follows;

$$\frac{\varepsilon_b A \rho_a}{\dot{m}_a} \frac{\partial T_a}{\partial t} + \frac{\partial T_a}{\partial z} = (C_v h_m (w_a - w_s) - h) \frac{a_s A}{\dot{m}_a C_a} (T_a - T_s) + \left(\frac{a_s f}{2 C_a}\right)\left(\frac{G_a}{\rho_m \varepsilon_b^{3/2}}\right)^2 \tag{13}$$

The energy conservation equation for the desiccant particle, using solid side resistance can be presented as

$$\frac{k_s}{r^2}\frac{\partial}{\partial r}\left(r^2\frac{\partial T_s}{\partial r}\right)=\rho_s C_s\frac{\partial T_s}{\partial t}-H_A\rho_s\frac{\partial q}{\partial t} \tag{14}$$

where, $\rho_S$ is the silica gel particle density and $C_s$ is the specific heat of silica gel as a function of its water content (Pesaran and Mills [16]). In Eq. (14), air temperature inside pores is assumed to be equal to that of desiccant temperature. Eqs. (13) and (14) are coupled by the continuity at the particle surface as follow

$$k_s\frac{\partial T_s}{\partial r}\Big)_{r=D_p/2}=h_c(T-T_s) \tag{15}$$

The second boundary condition for Eq. (14) is

$$k_s\frac{\partial T_s}{\partial r}\Big)_{r=0}=0 \tag{16}$$

Using the lumped capacitance model for the energy balance in the bed gives

$$k_b\frac{\partial^2 T_s}{\partial z^2}+H_A h_m a_s(w_a-w_s)-ha_s(T_s-T_a)=C_b\rho_s(1-\varepsilon)\frac{\partial T_s}{\partial t} \tag{17}$$

where, $C_b$ is the specific heat capacity of the desiccant bed (Chakraborty et al. [20,21]) and is assumed to be the same as $C_s$ of Pesaran and Mills [16]. In Eq. (17), first term is the axial conduction effect, the second term is the heat generated due to enthalpy of adsorption, and the third term is the convection heat transfer to or from flowing air stream. This equation has the initial condition as

$$T_{s(z,t=0)}=T_{s0} \tag{18}$$

Finally, for the gas phase side Eqs. (5) and (13), initial and boundary conditions are as follows

$$T_{a(z,t=0)}=T_{a0},\quad w_{a(z,t=0)}=w_{a0},\quad T_{a(z=0,t)}=T_{ai}\quad\text{and}\quad w_{a(z=0,t)}=w_{ai} \tag{19}$$

This completes the system of equations for heat and mass transfer through adsorption as well as desorption processes in a desiccant bed, with and without cyclic operation.

Practically, the physical process of adsorption is so fast relative to other steps like diffusion within silica gel particles, that in and near the silica gel particles, a local equilibrium exists. Kafui [18] concluded that the lumped capacitance model is acceptable for small particle diameters, hence this study also uses the lumped capacitance model to predict the performance of the desiccant bed by semi-analytical approach. The flow direction of air in the packed bed is in one direction i.e. $z$ –axis. The heat and mass transfer takes place only by forced convection to or from the flowing air through the bed and the heat transferred by conduction compared to heat transferred by convection is neglected (San and Jiang [15], Pesaran and Mills [16] and Kafui [18]). The radial dispersion is regarded as unimportant when the bed diameter is far greater than the particle diameter (Yang [9]). For relatively high air velocity the vertical heat conduction and moisture dispersion can be neglected, and a single film mass transfer coefficient controls the transfer rate between the flowing air and the silica gel particles. Since the air enters and leaves the bed continuously, the steady state forms of Eqs. (5) and (13) are used. San and Jiang [15] included that the friction effect in the packed bed is very small compared with the adsorption/ desorption heats and can be neglected for small as well as high air velocities. For these assumptions the general model can be reduced to the lumped capacitance model and gives the following reduced model

$$\frac{\partial w_a}{\partial z}=-\frac{h_m a_s A}{\dot m_a}(w_a-w_s)(1-w_a) \tag{20}$$

$$\frac{\partial T_a}{\partial z}=(C_v h_m(w_a-w_s)-h)\frac{a_s A}{\dot m_a C_a}(T_a-T_s) \tag{21}$$

$$C_s\rho_b\frac{\partial T_s}{\partial t}+ha_s(T_s-T_a)=H_A h_m a_s(w_a-w_s) \tag{22}$$

along with Eq. (10) for the solid phase mass balance. Now, the transient heat and moisture transfer process is described by Eqs. (10), (20), (21) and (22) in addition to Eq. (2)

## 3. Semi-analytical model derivation

The main idea of using quasi-steady state assumption for the proposed semi-analytical method can be explained as follows. At a given time $t$ the bed water content $q_{(z,t)}$ and temperature $T_{s(z,t)}$ are assumed to be constants for the bed height increment $dz$. Hence, the governing equations for gas phase (Eqs. (20) and (21)) are differential equations with respect to $z$-direction. And for a given location $z$, the air properties on the boundaries of the bed control volume are assumed to be constants for a time interval $dt$(*i.e.* $w_{a(z,t)}=w_{a(z,t+dt)}$ and $T_{a(z,t)}=T_{a(z,t+dt)}$). Hence, the governing equations for solid phase (Eqs. (10) and (22)) are differential equations with respect to time only.

Rearranging Eq. (20)

$$\int_{w_{a(z)}}^{w_{a(z+\Delta z)}}\frac{dw_a}{(w_a-w_s)(1-w_a)}=\int_z^{z+\Delta z}\frac{h_m a_s A}{\dot m_a}\partial z \tag{23}$$

Integrating Eq. (23) for the pre-described limits leads to a relation for exit air humidity and is given by

$$w_{a(z+\Delta z)}=\frac{w_{s(z)}(1-w_{a(z)})+(w_{a(z)}-w_{s(z)})\exp(-NTU_m(1-w_{s(z)}))}{(1-w_{a(z)})+(w_{a(z)}-w_{s(z)})\exp(-NTU_m(1-w_{s(z)}))} \tag{24}$$

where, $NTU_m$ is the number of mass transfer units

$$NTU_m=\frac{h_m a_s A\Delta z}{\dot m} \tag{25}$$

And is proportional to the mass transfer coefficient, area of mass transfer, and inversely proportional to air mass flow rate. Neglecting the flow friction effect, Eq. (21) is written as

$$\int_{T_{a(z)}}^{T_{a(z+\Delta z)}}\frac{\partial T_a}{(T_a-T_s)}=\int_z^{z+\Delta z}(C_v h_m(w_a-w_s)-h)\frac{a_s A}{\dot m_a C_a}\partial z \tag{26}$$

Substituting $(w_a-w_s)$ from Eq. (20) in Eq. (26), and defining $\xi=NTU_h/C_a\Delta z$, a relation for exit air temperature is found and this is given by,

$$\frac{T_{a(z+\Delta z)}-T_{s(z)}}{T_{a(z)}-T_{s(z)}}=\left(\frac{1-w_{a(z+\Delta z)}}{1-w_{a(z)}}\right)^{-\frac{C_v}{C_a}}\exp(-\xi\Delta z) \tag{27}$$

Without neglecting the effect of the flow friction, Eq. (26) will be replaced with

$$\frac{\partial(T_a-T_s)}{\partial z}+(h-C_v h_m(w_a-w_s))\frac{a_s A}{\dot m_a C_a}(T_a-T_s)=\left(\frac{a_s f}{2C_a}\right)\left(\frac{G_a}{\rho_m\varepsilon_b^{3/2}}\right)^2 \tag{28}$$

Eq. (28) is a first order differential equation and has the solution as follows

$$T_{a(z+\Delta z)}-T_{s(z)}=\frac{\chi_2}{\chi_1^2}+\left[(T_{a(z)}-T_{s(z)})-\frac{\chi_2}{\chi_1^2}\right]\exp(-\chi_1) \tag{29}$$

where the parameters $\chi_1$ and $\chi_2$ are as follows

$$\chi_1 = \left(\frac{NTU_h}{C_v} - NTU_m(w_{aav} - w_{s(z)})\right)\frac{C_v}{C_a} \tag{30}$$

$$\chi_2 = \left(\frac{a_s f}{2C_a}\right)\left(\frac{G_a \Delta z}{\rho_m \varepsilon_b^{3/2}}\right)^2 \tag{31}$$

And $NTU_h$ is the number of heat transfer units

$$NTU_h = \frac{h a_s A \Delta z}{\dot{m}} \tag{32}$$

For Eq. (10)

$$\int_{q_{(t)}}^{q_{(t+\Delta t)}} dq = \int_t^{t+\Delta t} \frac{h_m a_s}{\rho_b}(w_{aav} - w_{s(z)})dt \tag{33}$$

where, $w_s$ is a function of bed temperature and water content. However, in this study, it is assumed to be constant for a small increment of time. Hence, Eq. (33) can be integrated and gives

$$q_{t+\Delta t} - q_t = \varphi_1(w_{aav} - w_{s(z)})\Delta t \tag{34}$$

where $\phi_1 = a_s h_m/\rho_b$. Finally, for Eq. (22), it can be rearranged as a first order differential equation, defining $\phi_2 = h a_s/C_s\rho_b$ and $\phi_3 = H_A h_m/h$ the solution is as follows

$$T_{s(t+\Delta t)} - T_{s(t)} = \frac{\varphi_3(w_{aav} - w_{s(z)})}{\varphi_2} + \left((T_{s(t)} - T_{aav}) - \frac{\varphi_3(w_{aav} - w_{s(z)})}{\varphi_2}\right)\exp(-\varphi_2 \Delta t) \tag{35}$$

Hamed [22] assumed that the properties of flowing air are constant through the desiccant bed. This assumption aids in obtaining analytical solution for the solid phase moisture balance equation. Using same criteria, for small increments of time and space, Eqs. (24), (27), (29), (34) and (35) are the analytical solution for the governing Eqs. 10 and (20)–(22). Therefore, dividing the bed into a number of layers and the time of operation into number of time intervals it is possible to evaluate the performance of the bed. A computer program using C++ language is developed for solving these four equations simultaneously for total bed height and total time of operation.

## 4. Numerical procedure

The set of coupled nonlinear partial differential Eqs. (20), (21) are solved by Runge Kutta Fehlberg method (Lee and Schiesser [23]) with prescribed boundary conditions as given by Eq. (19). Eqs. (10) and (22) are solved by forward finite difference scheme with initial conditions given by Eqs. (11) and (18). A computer program is developed to solve numerically the above described set of equations and the results are compared with the results obtained using the semi-analytical model. A time step of 0.01 s and a grid size of less than 1.0 mm with total 100 grid points are used in the simulation to ensure numerical stability and accuracy. When the grid size is less than or equal to 1.0 mm, the simulation results are independent of the grid size.

The calculation procedure for solving Eqs. 10, 20, 21 and 22 numerically is summarized as follow:

(1) Set the total time of operation and bed design parameters $(L, d_b, d_p)$.
(2) Set the flowing air properties $(v, T_{ai}, w_{ai})$ and bed properties $(T_{s0}, q_0)$.
(3) Set the grid size and time step size ($\Delta z$ and $\Delta t$).
(4) For the current incremental volume ($i = 1$) assume $w^j_{a(i+1)}$ and $T^j_{a(i+1)}$
  i Calculate $C_p$(equation A4), $C_s$(equation A3), $h$ and $h_m$(equations (A1and A2)), $H_A$ (equation A5), $f$ (equation A8) and$w_s$(equations A6 and A7).
  ii Use Runge Kutta Fehlberg method to calculate $w^{j+1}_{a(i+1)}$ and $T^{j+1}_{a(i+1)}$ from Eqs. (20) and (21) respectively.
  iii Use forward scheme finite difference method to calculate $q_{(i,t+dt)}, T_{s(i,t+dt)}$ from Eqs. (10) and (22) respectively.
  iv Calculate the errors $\left(\left|w^{j+1}_{a(i+1)} - w^j_{a(i+1)}\right| \text{and} \left|T^{j+1}_{a(i+1)} - T^j_{a(i+1)}\right|\right)$
  v Repeat steps (i) to (iv) until errors are $\leqslant 1.0^{-10}$
(5) Repeat step (4) for $i = 2, 3 \ldots n$
(6) Set the new values of bed water content and temperature $q_{(i,t)}$ and $T_{s(i,t)}$.
(7) Repeat steps (4) to (6) until the completion of the total time of operation. The output is printed in between steps number Eq. (5) and Eq. (6).

## 5. Model validation

The results of the suggested semi-analytical model are compared with the experimental investigations of references 17 and 18. These experiments include adsorption and desorption processes for regular and intermediate density of silica gels. Table 1 lists the data of some experiments from reference 17. The inside diameter of the bed considered in these experiments is 0.13 m and the height is less than 0.15 m to avoid pressure drop effects. Silica gel particles with diameters of 2.54, 3.88 and 5.2 mm have been used for various runs as listed in Table 1. Also, the time of successful experiment is about 30 min which is typical of a practical operation. In addition, Kafui [18] conducted the heat and moisture transfer experiments for a square matrix of silica gel particles with parallel passages. In this work, some modifications are applied to the mathematical model for simulating these experimental data (Kafui [18]). These data are furnished in Table 2.

## 6. Results and discussion

The discussion that follows will elaborate upon, how well the results of the semi-analytical model and numerical model compare with the experimental results reported by Pesaran and Mills [17] and Kafui [18]. In addition to this, the stability of the semi-analytical model will be highlighted and mechanisms of adsorption and desorption processes will be investigated.

**Table 1**
Bed and flow conditions for experiments conducted by Pesaran and Mills [17].

| Run | Gel type | Process kind | $d_p$ [mm] | $L$ [cm] | $q_0$ [kg $_w$/kg $_s$] | $T_{s0}$ [°C] | $T_{ai}$ [°C] | $w_{ai}$ [kg $_v$/kg $_a$] | $v$ [m/s] | $t$ [sec] |
|---|---|---|---|---|---|---|---|---|---|---|
| 1 | RD | Des | 5.2 | 5.0 | 0.26 | 25.4 | 25.4 | 0.0007 | 0.67 | 1200 |
| 2 | RD | Des | 5.2 | 5.0 | 0.368 | 25.0 | 25.0 | 0.0051 | 0.4 | 1800 |
| 3 | RD | Ads | 3.88 | 7.75 | 0.0417 | 23.3 | 23.3 | 0.01 | 0.21 | 1800 |
| 4 | RD | Ads | 2.54 | 6.5 | 0.041 | 24.7 | 24.7 | 0.0106 | 0.39 | 1800 |
| 5 | RD | Des | 5.2 | 5.0 | 0.37 | 23.8 | 23.5 | 0.009 | 0.65 | 1200 |
| 6 | RD | Ads | 5.2 | 5.0 | 0.0668 | 25.6 | 25.6 | 0.01093 | 0.4 | 1800 |
| 7 | ID | Ads | 3.88 | 7.75 | 0.005 | 24.4 | 24.4 | 0.0063 | 0.67 | 1200 |
| 8 | ID | Ads | 3.88 | 7.75 | 0.0088 | 23.7 | 23.7 | 0.0097 | 0.45 | 1200 |

**Table 2**
Silica gel matrix design specifications (Kafui [18]).

| Matrix | Gel type | Process kind | $d_p$ [mm] | $L$ [cm] | $p$ [mm] | $A$ [m$^2$] | $q_0$ [kg $_w$/kg $_s$] | $T_{s0}$ [°C] | $T_{ai}$ [°C] | $w_{ai}$ [kg $_v$/kg $_a$] | $v$ [m/s] | $t$ [sec] |
|---|---|---|---|---|---|---|---|---|---|---|---|---|
| 1-A | ID | Ads | 0.1 | 10.16 | 0.9 | 0.0956 | 0.07486 | 35.32 | 35.62 | 0.01603 | 1.304 | 631 |
| 2-B | ID | Ads | 0.1 | 10.16 | 2.0 | 0.0924 | 0.13505 | 38.02 | 35.83 | 0.01899 | 1.443 | 421 |

**Table 3**
Root of mean square of relative errors.

| Run | Numerical | | Semi-analytical | |
|---|---|---|---|---|
| | $\delta(w_a)$[%] | $\delta(T_a)$[%] | $\delta(w_a)$[%] | $\delta(T_a)$[%] |
| 1 | 7.72 | 13.92 | 3.79 | 11.78 |
| 2 | 19.42 | 7.72 | 21.23 | 7.10 |
| 3 | 11.51 | 5.56 | 12.29 | 5.39 |
| 4 | 32.84 | 5.00 | 27.17 | 3.31 |
| 5 | 5.88 | 2.53 | 6.61 | 2.24 |
| 6 | 25.79 | 2.95 | 22.18 | 3.04 |
| 7 | 24.25 | 6.33 | 25.71 | 6.32 |
| 8 | 19.42 | 7.72 | 21.23 | 7.10 |
| 1-A | 25.08 | 12.18 | 23.64 | 11.72 |
| 2-B | 11.07 | 2.18 | 10.76 | 2.47 |

Results of adsorption processes are shown in Figs. 2–8. It can be observed that from the figures the adsorption process is characterized by an initial sharp rise in both temperature and humidity ratio of the exit air. The temperature curve reaches its peak generally within 0.2 relative time and then decreases at a more gradual rate depending on the air flow rate. However the time required for the air temperature to reach its peak depends strongly on the air flow rate, for high flow rates the peak is observed to be within 0.05 relative time (Figs. 2 and 3) and for lower flow rates it is at 0.2 relative time (Fig. 4). The temperature rise in the outlet air results from the initial high rate of adsorption which is accompanied by high rate of heat of adsorption which rises the temperature of bed particles and consequently heating up the flowing air by means of convective heat transfer. As the temperature of bed increases, its adsorptive capacity decreases sharply and the released heat of adsorption falls, this leads to the peak in exit air temperature response curve (Figs. 2–8).

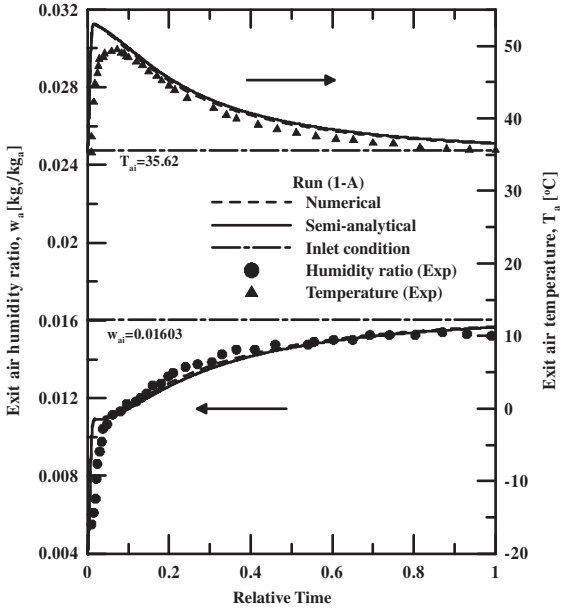


**Fig. 2.** Comparison of the time history of exit air humidity ratio and temperature for Run (1-A) obtained using semi-analytical, numerical and experimental procedures.

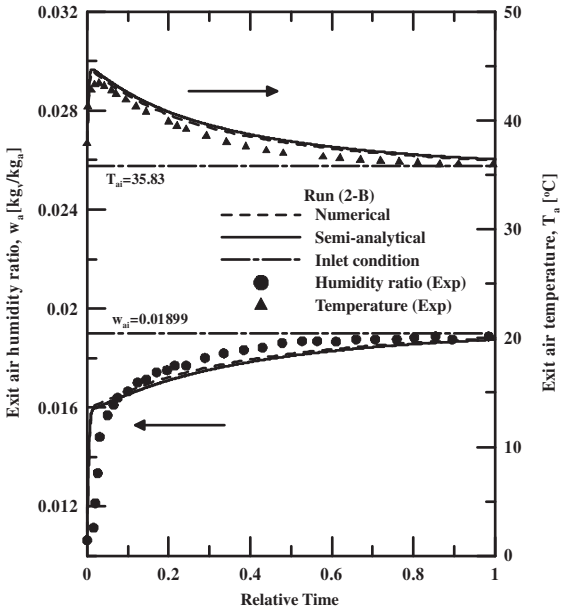


**Fig. 3.** Comparison of the time history of exit air humidity ratio and temperature for Run (2-B) obtained using semi-analytical, numerical and experimental procedures.

Again following Figs. 2–8, during the start of adsorption operation the bed adsorption capacity is high. For small fraction of relative times, the exit air humidity ratio is very minimal and, then there is a sudden increase in its value. The sharp rise in the exit air humidity ratio during early relative time of bed operation occurs ahead of the relative time for peak rise in exit air temperature, (Figs. 4–6). Continuing the adsorption process, the bed water content slowly rises and bed adsorptivity decreases gradually which explains the gradual increase in the exit air humidity ratio response curves, starting from 0.05 relative time for high flow rates (Figs. 2, 3), 0.1 for medium flow rates (Figs. 5–8) and 0.2 for low flow rates (Fig. 4).

In the desorption tests, the exit air humidity ratio and temperature curves have an inverse trend in comparison to the adsorption tests. Generally, the maximum exit air humidity and temperature is recorded at 0.0 relative time. Then a sharp decrease in both temperature and humidity ratio of the exit air occurs. The temperature curve reaches its dip generally within 0.15 relative time (Figs. 9–11), then increases subsequently at a more gradual rate. The sharp decrease in air temperature response curve results from the initial high rate of desorption which is accompanied by high extraction rate of heat of desorption from the bed particles which cools the bed and consequently cools the flowing air by means of convective heat transfer. As the temperature of bed decreases, the desorption rate decreases sharply and corresponding heat of desorption reduces, this leads to the dip in exit air temperature response curve (Figs. 9–11).

During the desorption process, it is to be observed that the response of air humidity ratio has a high negative slope when compared to air temperature response curve. The slope of the humidity ratio response curve falls sharply prior to the dip in exit air temperature response curve as a result of the fall in the desorption rate

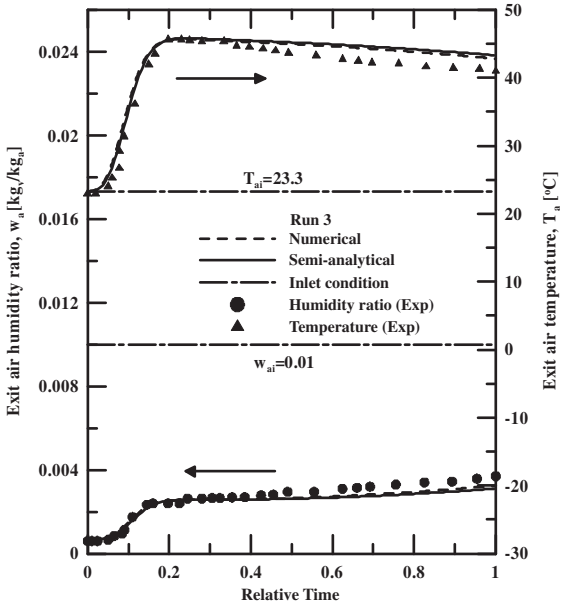


**Fig. 4.** Comparison of the time history of exit air humidity ratio and temperature for Run (3) obtained using semi-analytical, numerical and experimental procedures.

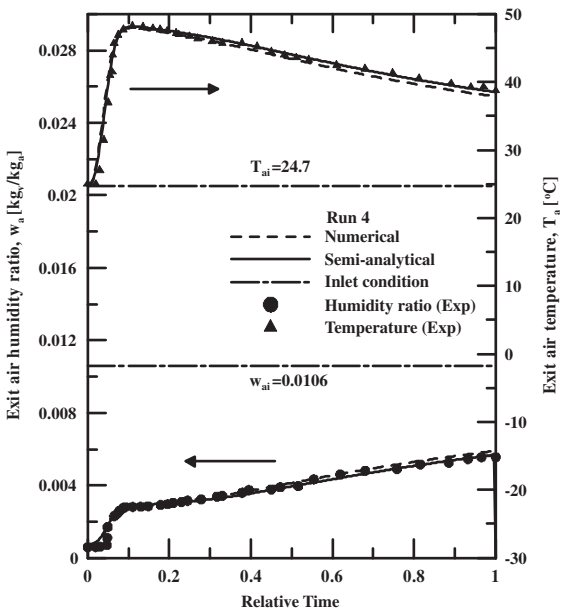


**Fig. 5.** Comparison of the time history of exit air humidity ratio and temperature for Run (4) obtained using semi-analytical, numerical and experimental procedures.

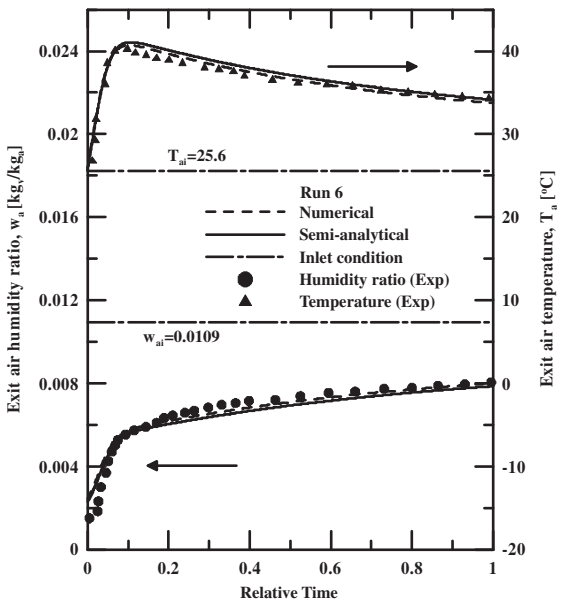


**Fig. 6.** Comparison of the time history of exit air humidity ratio and temperature for Run (6) obtained using semi-analytical, numerical and experimental procedures.

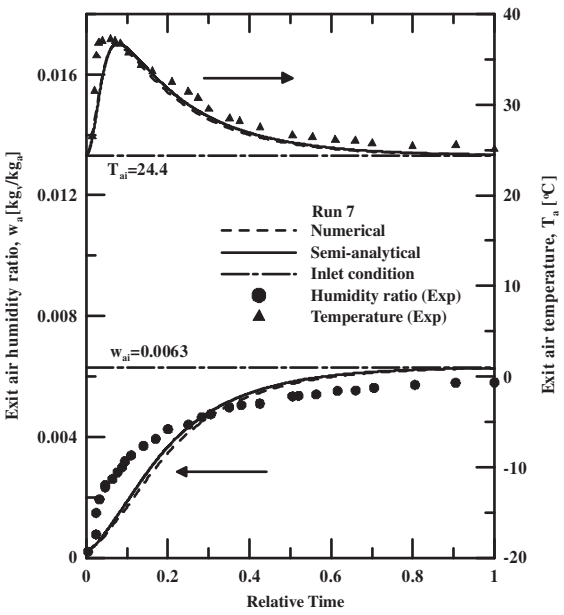


**Fig. 7.** Comparison of the time history of exit air humidity ratio and temperature for Run (7) obtained using semi-analytical, numerical and experimental procedures.

because of sharp decrease in the system temperature. With progressing time, and starting from 0.15 relative time, the temperature of exit air increases and humidity ratio decreases gradually as observed in Figs. 9–11. For very long time of operation, the bed and the flowing air should achieve the equilibrium state. Under equilibrium, the vapor pressure of the flowing air and the vapor pressure on the particles surface will be equal. Consequently, no heat of adsorption will be released and the temperature and humidity of the exit air will remain the same as that at inlet.

For adsorption processes, a good agreement is found for the results obtained using both semi-analytical and numerical models with the experimental data as in Figs. 2–6, however the agreement is less in case of ID silica gel as observed from Figs. 7 and 8. On the other hand, the agreement is not encouraging for desorption processes as in Figs. 9–11. However, the agreement between the numerical results and semi-analytical results holds good for all runs (Figs. 2–11).

With a view to compare the results obtained using the numerical and semi-analytical models, the root of mean square of relative errors ($\delta(X)$) has been calculated using Eq. (36). In Eq. (36), $X$ refers to air humidity ratio $w_a$ and temperature $T_a$. The root of mean square of relative errors of air humidity ratio $\delta(w_a)$ and exit air temperature $\delta(T_a)$ for the experimental runs have been evaluated and detailed in Table 3.

$$\delta(X) = \sqrt{\frac{\sum_{i=1}^{n}\left(\frac{X_{exp}-X_p}{X_{exp}}\right)^2}{n}} \tag{36}$$

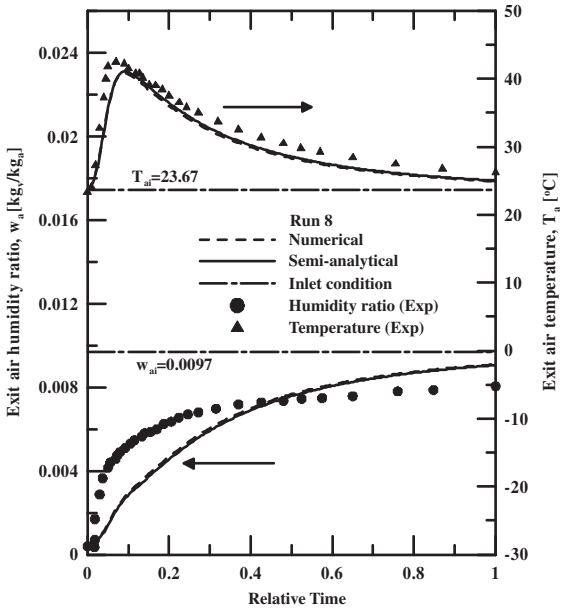


**Fig. 8.** Comparison of the time history of exit air humidity ratio and temperature for Run (8) obtained using semi-analytical, numerical and experimental procedures.

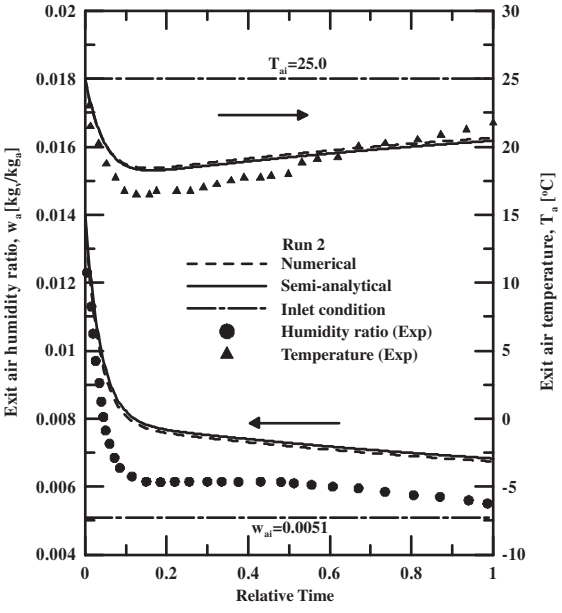


**Fig. 10.** Comparison of the time history of exit air humidity ratio and temperature for Run (2) obtained using semi-analytical, numerical and experimental techniques.

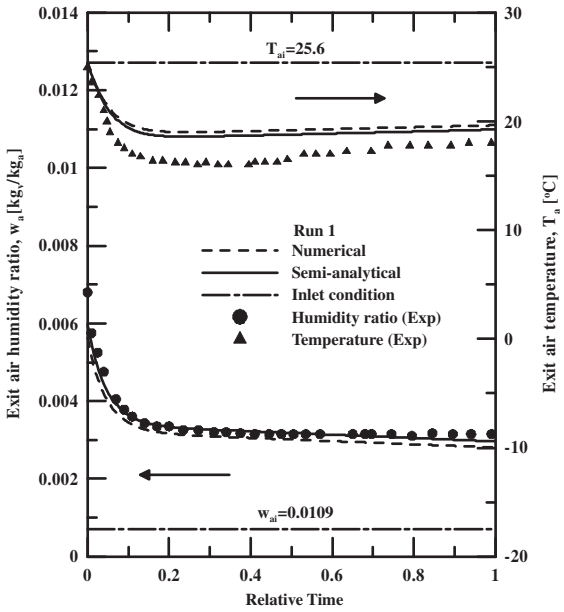


**Fig. 9.** Comparison of the time history of exit air humidity ratio and temperature for Run (1) obtained using semi-analytical, numerical and experimental techniques.

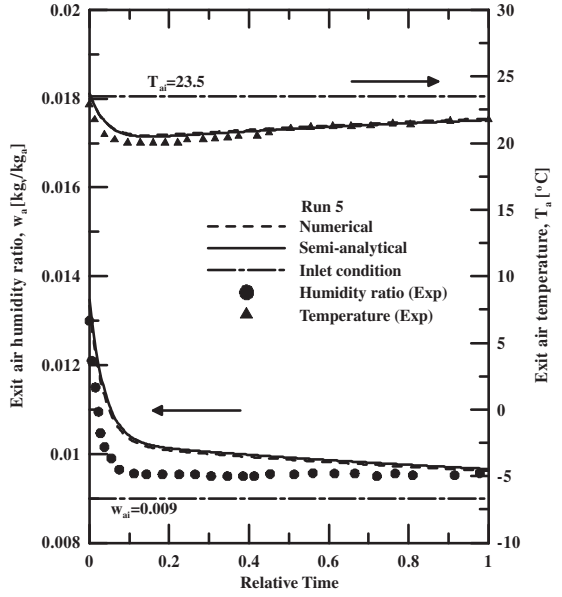


**Fig. 11.** Comparison of the time history of exit air humidity ratio and temperature for Run (5) obtained using semi-analytical, numerical and experimental techniques.

It is observed from Table 3 that, the minimum mean square root of relative errors is 3.79% for exit air humidity ratio and 2.24% for exit air temperature in case of semi-analytical model. In case of numerical model, the smallest roots of mean square of relative errors are 5.88% and 2.18% respectively for exit air humidity ratio and temperature. Similarly, maximum roots of mean square of relative errors for exit air humidity ratio are 27.17% and 32.84%, for exit air temperature it is 11.78% and 13.92 respectively for semi-analytical and numerical models. For runs 2, 3, 5, 7 and 8, it is observed that numerical model provides good estimates for the exit air humidity ratio but the semi-analytical model provides good results for exit air temperature compared to the numerical model. For experimental runs 6 and 2-B, the root of mean square of relative errors on exit air humidity ratio from semi-analytical model are less when compared to numerical model. For the same experiments the root of mean square of relative errors on exit air temperature is high for semi-analytical model when compared to numerical model. For experiments 1, 4 and 1-A it is observed that semi-analytical results have less errors for both exit air humidity ratio and temperature. From this detailed comparison, it can be stated that the proposed semi-analytical solution can be used to predict the behavior of a silica gel packed bed during adsorption or desorption process.

The effect of time as well as space increments sizes on the degree of agreement between semi-analytical results and the experimental data is shown in Figs. 12 and 13. The semi-analytical model results have been calculated for various velocity ratios $\Psi = 1.0, 0.5, 0.33, 0.25, 0.2, 0.1, 0.05$ and $0.01$ where $\Psi = (\Delta z/\Delta t)/v$ and time step is fixed at $\Delta t = L/v$. From Fig. 12, it can be seen that

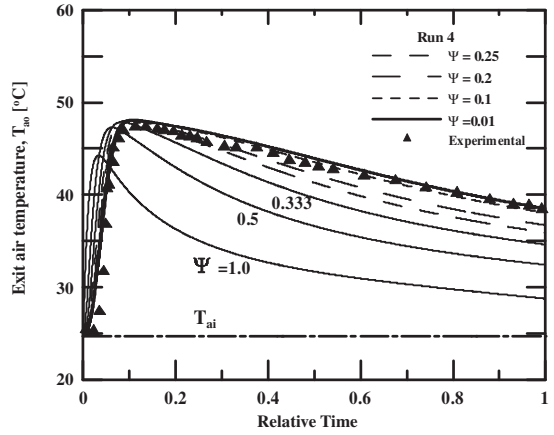


**Fig. 12.** Influence of velocity ratio on the exit air temperature with progressing time (run 4).

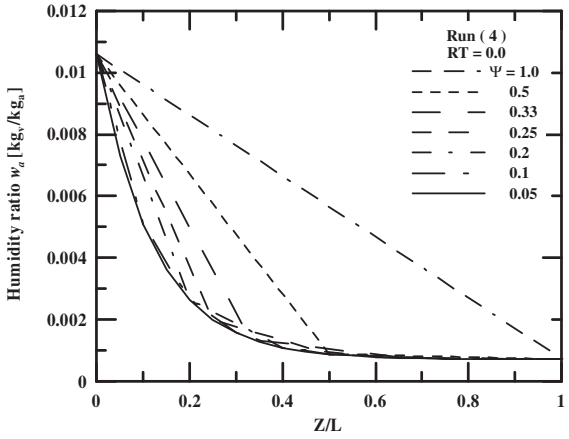


**Fig. 14.** Influence of velocity ratio on the axial variation of air humidity ratio for run 4 at relative time 0.0.

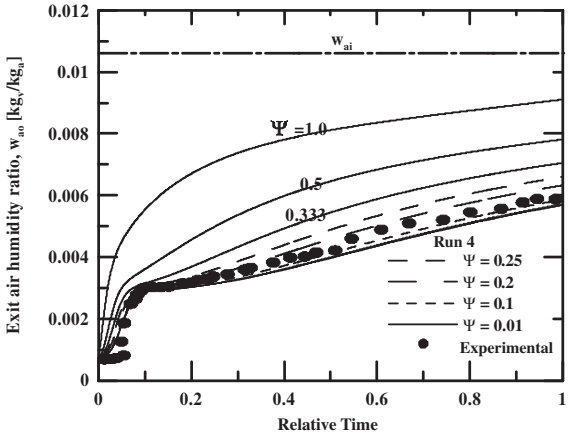


**Fig. 13.** Influence of velocity ratio on the exit air humidity ratio with progressing time (run 4).

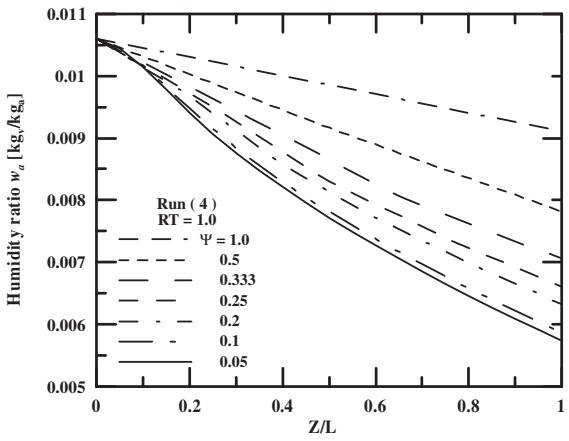


**Fig. 15.** Influence of velocity ratio on the axial variation of air humidity ratio for run 4 at relative time 1.0.

there is no significant difference in the results of outlet air temperature when $\Psi$ is maintained less than or equal to 0.05 ($\Psi \leqslant 0.05$) and the same holds true for outlet air humidity ratio (Fig. 13).

The discrepancy of results using $\Psi = 1.0$, 0.5 and 0.33 can be attributed to the fact that, the integration interval (or limits of integration) for Eqs. (20) and (21), ($\Delta z$), is quite wide which can mean that the integration results obtained have not been able to consider the axial bed water content and temperature distributions. Further, it is noticed that when bed increments are made small or the limits of integration are brought closer by choosing $\Psi = 0.1$, 0.05 and 0.01, the results for Eqs. (20) and (21) do improve and agree well with experimental results. Figs. 14 and 15 show the change in air humidity ratio along the axial position in the bed for relative times of 0.0 and 0.1, respectively. It can be observed that, exit air humidity ratio ($z/L = 1.0$) at 0.0 relative time is independent of velocity ratio (Fig. 14). This is because of the uniform distribution of bed water content and temperature at the start of the process. And continuing the process the axial distribution of bed water content and temperature are no more uniform, which results in the high discrepancy in the exit air humidity ratio (Fig. 15).

Figs. 16 and 17 show the effect of velocity ratio on the results for runs (1) and (6). Run (1) is desorption process and run (6) is adsorption process. It can be observed that, for a velocity ratio $\Psi = 0.1$ the solution is stable (that is the semi-analytical solution results agree will with the experimental data (Pesaran and Mills [17]). It is interesting to note that the magnitude of velocity ratio coincides with the

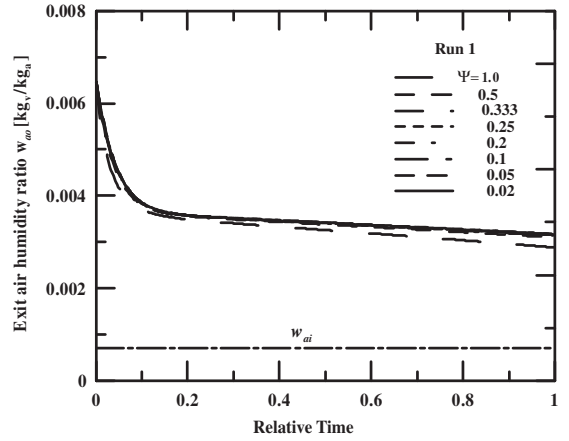


**Fig. 16.** Variation of exit air humidity ratio with time for different velocity ratios for run 1.

ratio $d_p/L$ which is also equal to 0.104. Hence, when semi-analytical solution approach is used, for a stable solution it is sufficient to divide the bed, to obtain bed increment size, such that the velocity ratio is equal to $d_p/L$ for a time increment size of $L/v$. Similar observations are true for the runs listed in Tables 1 and 2.

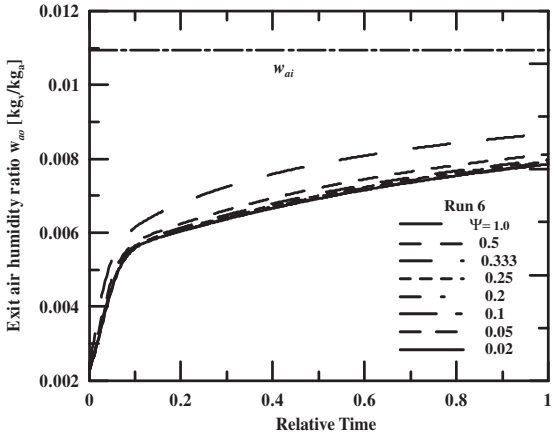


**Fig. 17.** Variation of exit air humidity ratio with time for different velocity ratios for run 6.

## 7. Conclusions

A transient analysis of heat and mass transfer during adsorption and desorption processes in a vertical silica gel packed bed has been developed. Lumped capacitance model is adopted for the energy balance as well as for moisture balance equations. A new semi-analytical model is derived. With an intention to compare the results of semi-analytical model apart from the experimental results, numerical schemes of Runge–Kutta Fehlberg and forward scheme finite difference techniques are also being attempted. The results of semi-analytical and numerical models agree well with the experimental results for both desorption and adsorption processes. From the stability analysis it is found that semi-analytical model results agree well with the experimental ones only when the limits of integration with respect to spatial coordinate is such that it should embody the influence of axial bed water content and temperature distributions. Interestingly, this condition is found to be achieved when the velocity ratio is equal to the ratio of particle diameter to the bed length. Using the proposed semi-analytical model, the root of mean square of relative errors for exit air temperature ranges between 2.24% and 11.78% and for exit air humidity the error range is between 3.79% and 27.17%. These figures, when compared with those of numerical model, indicate the validity of the semi-analytical model to predict the bed behavior during adsorption and desorption processes.

## Acknowledgements

The authors are highly pleased and thank the reviewer(s) for devoting their time and effort in reviewing this article. The technical depth of this article has raised enormously due to reviewer(s) valuable inputs.

## Appendix A

A1. Mass transfer coefficients [16] $h_m = 0.704 G_a Re^{-0.51}$

A2. Heat transfer coefficient [16] $h = 0.683 G_a C_a Re^{-0.51}$

A3. specific heat of silica gel [16,18] $C_s = 4.178 \times q + 0.921$

A4. The specific heat of moist air $C_a = 1.884 \times w_a + 1.005(1 - w_a)$

A5. Heat of adsorption [15,16,18]

Intermediate density silica gel

$$H_A = 2095.0 - 300.0 \times q \quad q \leqslant 0.15$$
$$H_A = 2050 \quad q > 0.15$$

Regular density silica gel

$$H_A = 3500.0 - 13400.0 \times q \quad q \leqslant 0.05$$
$$H_A = 2950.0 - 1400.0 \times q \quad q > 0.05$$

A6. Adsorption isotherms [15,16,18] $RH[\%] = 100 \times (a_0 + a_1 q + a_2 q^2 + a_3 q^3 + a_4 q^4)$

Regular density silica gel

$$a_0 = 0.0078, \quad a_1 = -0.05759, \quad a_2 = 24.16554$$
$$a_3 = -124.478, \quad a_4 = 204.226$$

Intermediate density silica gel

$$a_0 = 0, a_1 = 1.235, \quad a_2 = 267.99, \quad q \leqslant 0.07$$
$$a_3 = -3170.7, \quad a_4 = 10087.16$$
$$a_0 = 0.3316, a_1 = 3.18, \quad a_2 = a_3 = a_4 = 0 \quad q > 0.07$$

A7. Air humidity ratio [17] $w = \frac{0.622 RH \times P_{sat}(T)}{P_{tot} - 0.378 RH \times P_{sat}(T)}$

A8. Fluid friction coefficient [15]

$$f = 19.336 Re^{-0.616} \quad 0 \leqslant Re < 200$$
$$= 1.478 Re^{-0.15} \quad 500 \leqslant Re < 5000$$
$$= 4.064 Re^{-0.313} \quad 200 \leqslant Re < 500$$

Volumetric surface area [m$^2$/m$^3$] [24] (see Table A1).

**Table A1**
Volumetric surface area [24].

| $d_p$[mm] | $\varepsilon$ (Bed porosity or void fraction) | | |
|---|---|---|---|
| | 0.3 | 0.4 | 0.5 |
| 5.08 | $a_s$ = 825 | 708 | 590 |
| 2.54 | 1650 | 1420 | 1180 |
| 1.27 | 3300 | 2830 | 2360 |

## References

[1] P. Cruz, J.C. Santos, F.D. Magalhaes, A. Mendes, Simulation of separation processes using finite volume method, Computers and Chemical Engineering 30 (2005) 83–98.
[2] I.A.A.C. Esteves, J.P.B. Mota, Simulation of a new hybrid membrane/pressure swing adsorption process for gas separation, Desalination 148 (2002) 275–280.
[3] K. Daou, R.Z. Wang, Z.Z. Xia, Desiccant cooling air conditioning: a review, Renewable and Sustainable Energy Reviews 10 (2006) 55–77.
[4] K. Sumathy, K.H. Yeung, Li Yong, Technology development in the solar adsorption refrigeration systems, Progress in Energy and Combustion Science 29 (2003) 301–327.
[5] D.S. Kim, C.A. Infante Ferreira, Solar refrigeration options- a state-of-the-art review, International Journal of refrigeration 31 (2008) 3–15.
[6] Kuei-Sen Chang, Hui-Chun Wang, Tsair-Wang Chung, Effect of regeneration conditions on the adsorption dehumidification process in packed silica gel beds, Applied Thermal Engineering 24 (2004) 735–742.
[7] K.C. Ng, H.T. Chua, C.Y. Chung, C.H. Loke, T. Kashiwagi, A. Akisawa, B.B. Saha, Experimental investigation of silica gel-water adsorption isotherm characteristics, Applied Thermal Engineering 21 (2001) 1631–1642.
[8] Hui T. Chua, Kim C. Ng, Anutosh Chakraborty, Nay M. Oo, Mohamed A. Othman, Adsorption Characteristics of silica gel + water systems, Journal of Chemical Engineering Data 47 (2002) 1177–1181.
[9] Ralph T. Yang, Gas separation by adsorption processes, Boston, 1987.
[10] Y.H. Ma, T.Y. Lee, Transient diffusion in solids with a bipore distribution, AIChE Journal 22 (1) (1976) 147–152.
[11] L.K. Lee, The kinetics of sorption in a biporous adsorbent particle, AIChE Journal 24 (3) (1978) 531–534.
[12] Cheng-Chin Ni, Jung-Yang San, Mass diffusion in a spherical micro-porous particle with thermal effect and gas-side mass transfer resistance, International Journal of Heat and Mass Transfer 43 (2000) 2129–2139.
[13] M.M. Awad, A.K. Ramzy, A.M. Hamed, M.M. Bekheit, Theoretical and experimental investigation on the radial flow desiccant dehumidification bed, Applied Thermal Engineering 28 (2008) 75–85.
[14] A.K. Ramzy, A.M. Hamed, M.M. Awad, M.M. Bekheit, Theoretical investigation on the cyclic operation of radial flow desiccant bed dehumidifier, Journal of Engineering and Technology Research 2 (2010) 96–11.
[15] J.Y. San, G.D. Jiang, Modeling and testing of a silica gel packed-bed system, International Journal of Heat and Mass Transfer 37 (1994) 1173–1179.

[16] A.A. Pesaran, A.F. Mills, Moisture transport in silica gel packed beds-I. Theoretical study, International Journal of Heat and Mass Transfer 30 (1987) 1037–1049.
[17] A.A. Pesaran, A.F. Mills, Moisture transport in silica gel packed beds-II. Experimental study, International Journal of Heat and Mass Transfer 30 (1987) 1051–1060.
[18] K.D. Kafui, Transient heat and moisture transfer in thin silica gel beds, ASME Heat Transfer Journal 116 (1994) 946–953.
[19] K. Kamiuto, S.A. Ermalina, Effect of desorption temperature on CO2 adsorption equilibria of the honeycomb zeolite beds, Applied Energy 72 (2002) 555–564.
[20] A. Chakraborty, B.B. Saha, S. Koyama, K.C. Ng, The specific heat capacity of a Single component adsorbent-adsorbate system, Applied Physics Letters 90 (171902) (2007) 1–3.
[21] A. Chakraborty, B.B. Saha, K.C. Ng, S. Koyama, K. Srinivasan, Theoretical Insight of Physical Adsorption for a single component adsorbent-adsorbate system: I. Thermodynamic Property Surfaces, Langmuir 25 (4) (2009) 2204–2211.
[22] Ahmed M. Hamed, Theoretical and experimental study on the transient adsorption characteristics of a vertical packed porous bed, Renewable Energy 27 (2002) 525–541.
[23] H.J. Lee, W.E. Schiesser, Ordinary and Partial Differential Equation Routines in C, C++, Fortran, Java, Maple, and MATLAB Florida -2004.
[24] Charles N. Satterfield, Thomas K. Sherwood, The Role of Diffusion in Catalysis, Addison- Wesley, 1963.